

## **Complex Principal Component Analysis of Medium-term Nearshore Geomorphology at North Sendai Coast, Japan**

Yusuke Uchiyama<sup>1</sup> and Yoshiaki Kuriyama<sup>2</sup>

### **Abstract**

Complex principal component analysis (CPCA) is applied to examine medium-term geomorphological behavior of an exposed sandy beach adjacent to a gigantic breakwater of the Port of Sendai located near a river mouth in the Sendai Coast, Japan, using a 12-year series of bathymetry survey data. The results of CPCA and conventional real-PCA demonstrate that erosion and subsequent accretion of the submerged terrace formed in front of the river mouth appear in the first mode of CPCA and have the most significant influence on the medium-term geomorphology of the study area. The first mode is mostly caused by northward alongshore sediment transport driven by wave energy flux, explained from the observed wave data. The second mode of CPCA demonstrates that the sediments previously discharged from the river return again into the nearshore region, and furthermore, the topography changes due to cross-shore sediment transport emerge in the third mode of CPCA.

### **Introduction**

The Sendai Coast directly facing the Pacific Ocean stretches approximately 60 km long. An extent of about 50 km including the study area is categorized to be a sandy beach segmented by three rivers. The predominant direction of longshore sediment transport (littoral drift) is reported northward according to the previous studies (e.g., Uda et al., 1990). Local erosion is known to have taken place on the sandy beach in the vicinity of the Port of Sendai (Tanaka, 1983). This erosion is believed to be caused by action of stem waves and reflected waves caused by an 1800-m long gigantic breakwater (Figure 1) constructed from 1970 to 1973 at the southern limit of the port (Morishita et al., 1995). Therefore beach nourishments have been conducted twice in 1974 and 1975 and a 250m-long side-mounted quay (a shore-parallel structure attached to the breakwater) was constructed from 1977 to 1982 near the shoreward end of the breakwater. Tanaka et al. (1995) reported that the depth of closure along the Sendai Coast may be 18m deep which is much deeper

---

<sup>1</sup> Senior Researcher, Littoral Drift Division, Port and Airport Research Institute, 3-1-1 Nagase, Yokosuka 239-0826, Japan, phone: +81-46-844-5045, fax: +81-46-841-9012, email: uchiyama@pari.go.jp

<sup>2</sup> Head, Littoral Drift Division, Port and Airport Research Institute, 3-1-1 Nagase, Yokosuka 239-0826, Japan, email: kuriyama@pari.go.jp

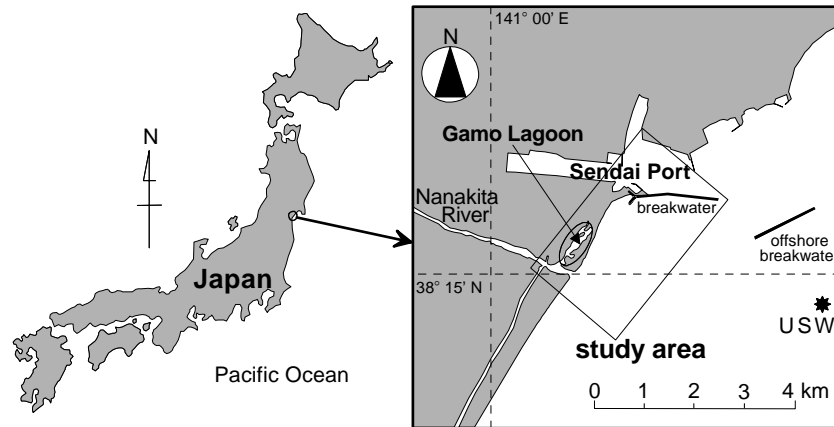


**Figure 1:** Location of the study. The slanting rectangle in the right panel approximately represents the area of the surveys, corresponding to the area from the breakwater of the Port of Sendai to the Nanakita River mouth. The caption “USW” indicates the location of the bottom-mounted ultrasonic wave gauge for offshore wave measurements.

than those in other coasts, suggesting that large-scale geomorphology and measurable offshore littoral transport may exist along the Sendai Coast. It can thus be summarized that there appears three distinctive geomorphic processes in the study site; 1) sediment discharge from the river resulting in stretch of sand spits and formation of an estuarine submerged terrace which influences on blockade of the river mouth (Tanaka et al, 1996), 2) interruption of the northward longshore sediment transport due to the port structures and 3) possible littoral process in offshore deeper regions.

Principal component analysis (PCA), which is also referred to as empirical eigenfunction analysis or empirical orthogonal function (EOF) analysis, has an primary advantage to statistically compress complicated variability, either in time and space, of the observed data set, the annually surveyed bathymetries here, into the fewest possible number of modes. This technique has been widely used for many of geophysical datasets including beach topography changes (e.g. Winant et al., 1975; Kuriyama, 2002). However, as pointed in the previous studies (e.g., Horel, 1984), the main drawback of PCA is its limitation to standing wave patterns, particularly since morphological changes are often related to propagating features. By contrast, complex PCA (CPCA), which has recently been applied to coastal morphological data (e.g., Liang and Seymour, 1991; Kuriyama and Lee, 2001; Ruessink et al., 2003), is know to be describable of not only standing waves, but also propagating waves in the observed data. Therefore it is strongly expected that CPCA is capable of identifying a coherent form that moves throughout the data, like longshore and cross-shore beach topography migrations and rapidly-moving bar-trough structures, which are essentially momentous for nearshore geomorphology.

In this manuscript, CPCA is adapted to a 12-year series of bathymetry dataset surveyed on the northern Sendai Coast, so as to clarify in an engineering time-scale,

To appear in Proceedings of Coastal Structure 2003, Portland, OR, USA, August 2003 (in print)  
medium-term geomorphology of the coast affected by the various factors interacting on its sediment budget, and to specify their causes by comparing the results of PCA and CPCA with potential forcing comprising surface waves and river discharges.

## Methods

### (1) Bathymetry survey

The hydrographic bathymetry surveys were performed 13 times annually in approximately every August since 1986 until 1998 for 12 years. The slanting rectangle in the right panel of Figure 1 represents the area of the surveys. The surveyed area covers a 3.35 km alongshore, from the 1800-m-long breakwater of the Port of Sendai to the south of the Nanakita River mouth, and a 1.80 km on-offshore, from the offshore region at the 18m water depth (i.e., D.L.-18.0m) to the backshore dune foot at D.L.+3.0m. Here, D.L. is the local datum level and is equivalent to the mean lower low water (MLLW) level of the area. The depth data is processed to be regularly spaced by 50 m alongshore and by 10 m on-offshore. Offshore waves measured at the point indicated by the caption "USW" in Figure 1 and discharges of the Nanakita River are also used in the analysis.

### (2) Description of complex and real principal component analysis

The three dimensional data matrix of the time-series horizontal bathymetries for 12 years,  $h(x', y', t)$ , is reduced into a quasi three-dimensional matrix,  $h(x, t)$ , by connecting each cross-shore profile one after another as expressed in Equation (1).

$$h(x', y', t) \rightarrow h(x, t). \quad (1)$$

This procedure enables us to conduct quasi three-dimensional PCA and CPCA readily as compared to the fully three-dimensional analysis (e.g., Bosma and Darlymple, 1996). It is quite simplistic but more informative than a set of two-dimensional PCA/CPCA applying to horizontal datasets (e.g., Liang and Seymour, 1991).

A converted scalar field,  $h(x, t)$ , where  $x$  and  $y$  denote spatial coordinates and  $t$  is time, can be described as Equation (2).

$$h(x, t) = \sum_{\omega} \{a(x, \omega) \cos \omega t + b(x, \omega) \sin \omega t\}, \quad (2)$$

where the Fourier coefficients,  $a(x, \omega)$  and  $b(x, \omega)$ , at a positive frequency  $\omega$  are defined in the usual manner. In terms of the complex representation of a variable, propagating features are commonly written as follows.

$$h(x, t) = \sum_{\omega} d(x, \omega) \exp(-i \omega t), \quad (3)$$

in which  $d(x, \omega) = a(x, \omega) + i b(x, \omega)$  and  $i = \sqrt{-1}$ . Expanding Equation (3) using the definition of  $c(x, \omega)$  yields

$$h(x, t) = \sum_{\omega} [\{a(x, \omega) \cos \omega t + b(x, \omega) \sin \omega t\} + i \{b(x, \omega) \cos \omega t - a(x, \omega) \sin \omega t\}]. \quad (4)$$

Equation (4) is also expressed as follows.

To appear in Proceedings of Coastal Structure 2003, Portland, OR, USA, August 2003 (in print)

$$H(x, t) = h(x, t) + i\tilde{h}(x, t) = H_{mn} \quad (5)$$

where  $H(x, t)$  is a complex bathymetry matrix and  $H_{mn}$  is the discrete form of  $H(x, t)$  at the  $m$ -th grid point and the  $n$ -th time step. The real parts of Equations (4) and (5) are simply the original data. The imaginary part,  $\tilde{h}(x, t)$  in Equation (5), called the Hilbert transform, represents a filtering operation upon  $h(x, t)$  in which the amplitude of each spectral density component is unchanged but its phase is advanced by  $\pi/2$ . The complex bathymetry  $H(x, t)$  accordingly contains phase information related to propagating waves in the data as well as its original information. The Hilbert transform  $\tilde{h}(x, t)$  can be obtained directly from a fast Fourier transform (FFT) routine:

$$\tilde{h}(x, t) = \sum_{\omega} W(\omega) \{b(x, \omega) \cos \omega t - a(x, \omega) \sin \omega t\}. \quad (6)$$

and  $W(\omega)$  is a filter weight at frequency  $\omega$ , set to be unity here, though.

Once a complex data matrix is generated, the eigenvalues and eigenvectors (i.e., eigenfunctions) of the complex covariance matrix are determined. The covariance matrix between the  $j$ -th and  $k$ -th position is written as:

$$B = [b_{jk}] = \frac{1}{N_x N_t} \sum_{n=1}^{N_x} H_{jn}^* H_{kn} \quad (7)$$

where  $N_x$  and  $N_t$  are numbers of the surveyed points and times of the surveys, and the asterisk \* denotes complex conjugation of the original matrix. The CPC approach compresses the information contained in the covariance matrix  $B$  into a relatively few complex eigenvectors and complex principal components. The conventional real PCA, by contrast, compresses the real correlation matrix  $A$  for the correlation between the  $j$ -th and  $k$ -th position, which can be calculated only from the real original data expressed in Equation (8), into real eigenvectors and real principal components.

$$A = [a_{jk}] = \frac{1}{N_x N_t} \sum_{n=1}^{N_x} h_{nj} h_{nk}. \quad (8)$$

In the actual calculation, the  $n$ -th eigenvalue  $\lambda_n$  and the  $n$ -th complex eigenvector  $u_n$  are defined as:

$$B \cdot u_n = \lambda_n u_n. \quad (9)$$

Since the covariance matrix is Hermitian, the eigenvalue  $\lambda_n$  is real. Using the following relation between the eigenvector and the  $n$ -th principal component at the  $k$ -th position:

$$(c_n)_k = \sqrt{\lambda_n N_x N_t} (u_n)_k, \quad (10)$$

an element  $(e_n)_j$  of the  $n$ -th complex eigenvector at the  $j$ -th position that contains the eigenvalue of  $\lambda_n$  is defined as:

$$(e_n)_j = \frac{1}{\lambda_n N_x N_t} \sum_{k=1}^{N_t} (c_n)_k H_{jk}^*. \quad (11)$$

To appear in Proceedings of Coastal Structure 2003, Portland, OR, USA, August 2003 (in print)

Finally the complex observation matrix of the bathymetry data  $H(x, t)$  is represented as a sum of the contributions from the  $n$ -th principal components:

$$H(x, t) = \sum_n e_n(x)^* \cdot c_n(t), \quad (12)$$

where the subscript  $n$  means that the variables  $c_n(t)$  and  $e_n(x)$  are the  $n$ -th principal components of the original data and elements of the eigenvectors. One may occasionally refer to  $e_n(x)$  and  $c_n(t)$  as the complex empirical orthogonal function (CEOF) or the complex empirical eigenfunction, and its temporal weighting.

Variance explained by the  $n$ -th principal component,  $r_n$ , to the total variation through the bathymetry data is defined with the eigenvalue and the trace of the covariance matrix  $B$  as:

$$r_n = \lambda_n / T_r(B). \quad (13)$$

Thus a mode with the largest value of the variance  $r_n$  exhibits the most significant topography change among all the modes detected by PCA and CPCA, called the first mode. The modes with the second and third largest variances are similarly called the second mode and the third mode.

One aspect of interest of PCA and CPCA is the ability to reconstruct the original data using empirical orthogonal functions (EOFs) and principal components. For the conventional real-PCA, the reconstructed data is reproduced from a full set of the components using real EOFs,  $e'(x)$ , and real temporal weightings (or real principal components),  $c'(t)$ , based on Equation (14).

$$h(x, t) = \sum_n e'_n(x) \cdot c'_n(t) = \sum_n h'_n(x, t), \quad (14)$$

where  $h'_n$  is a decomposed bathymetry explained by the  $n$ -th component. In CPCA, on the other hand, the observation matrix  $h(x, t)$  can not be directly rewritten as represented in Equation (14). However, since the real and imaginary parts of the complex bathymetry matrix  $H(x, t)$  are a Hilbert transform of one another, in theory, the real part can be considered alone (Horel, 1984; Lian and Seymour, 1991). Therefore it is possible to reconstruct the original data matrix  $h(x, t)$  using the complex conjugation of the CEOF and the complex principal components  $c(t)$ , by taking only the real part:

$$h(x, t) = \sum_n \text{real}\{e_n^*(x) \cdot c_n(t)\} = \sum_n h'_n(x, t). \quad (15)$$

It is frequently useful to reconstruct the bathymetry data using Equations (14) or (15) from a limited set of the components. The reconstructed data accounting for the  $n$ -th real principal component and the  $n$ -th complex principal component can be simply written as:

$$h'_n(x, t) = e'_n(x) \cdot c'_n(t) \quad (16)$$

$$h'_n(x, t) = \text{real}\{e_n^*(x) \cdot c_n(t)\} \quad (17)$$

in which the subscript  $n$  is again an integer denoting the mode number,  $h'_n(x, t)$  is a reconstructed bathymetry matrix based on the  $n$ -th real/complex eigenmode.

To appear in Proceedings of Coastal Structure 2003, Portland, OR, USA, August 2003 (in print)

Furthermore the reconstructed bathymetries described by Equations (16) to (17) can be rearranged into the original three-dimensional matrices by utilizing Equation (18).

$$h'_n(x, t) \rightarrow h'_n(x', y', t), \quad (18)$$

Therefore geomorphological features accounting for an arbitrary eigenmode can be visualized with the inversely-converted fully three-dimensional bathymetries.

## Results

### (1) Bathymetry survey

In order to examine overall geomorphology in the study area for the 12 years from 1986 to 1998, a temporally averaged bathymetry, root-mean-squares (R.M.S. or standard deviation) of bathymetry fluctuations and a trend distribution are calculated as respectively displayed in Figures 2 to 4. The trend is defined as a gradient of a time series plot of the bathymetry variations at each grid point determined with the linear least squares fitting. Positive values of the trend denote that the seabed elevates with time, or that accretion progresses there, whereas negatives represent local erosions. The nearshore isobathic lines align densely particularly in front of the river mouth, and the topography is varied more there. The trend demonstrates that this area and the offshore of the breakwater seem to be eroded, while accretion occurs at the landward of the breakwater.

Uda et al. (1990) estimated the depth of closure to be about 8m on the basis of the surveyed data obtained at about 25km south of the study site. Tanaka et al. (1995) examined the field data collected at about 10km south of the site, inferring that the depth of closure may reach up to about 18m. In the study area, the R.M.S. of the bed-elevation variations at the shallower area less than 10m deep is generally large. However, the R.M.S. is also larger near the breakwater and before the river mouth deeper than 10m, where the trend has non-zero values. The estimated depths of closure for these two area likely range from 13 to 14m near the breakwater and from 10 to 12m near the river mouth. This estimation is intermediate between two previous reports, implying that the analysis should be done through the whole domain including the offshore region. Therefore the following analysis is conducted for the entire surveyed-data shown in Figures 2 to 4.

### (2) Complex and real PCA

The variances explained by the first three modes are respectively 34.2%, 24.1% and 8.1% for PCA and 44.3%, 17.8% and 12.6% for CPCA. The cumulations for the first three modes are 66.4% for PCA and 74.7% for CPCA. This indicates that these three modes seem to mostly govern the geomorphology in the study area, and thus the following analysis is carried out using these three modes. The results of the first mode by the PCA and CPCA are displayed in Figures 5 and 6. The spatial distribution of the EOFs (empirical orthogonal functions),  $e_n(x)$ , derived from the

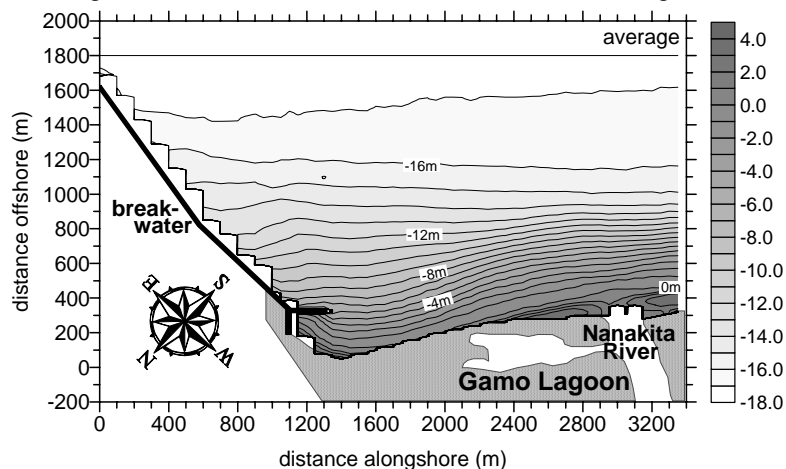


**Figure 2:** Temporally-averaged isobathic contours (contour intervals: 1.0 m).

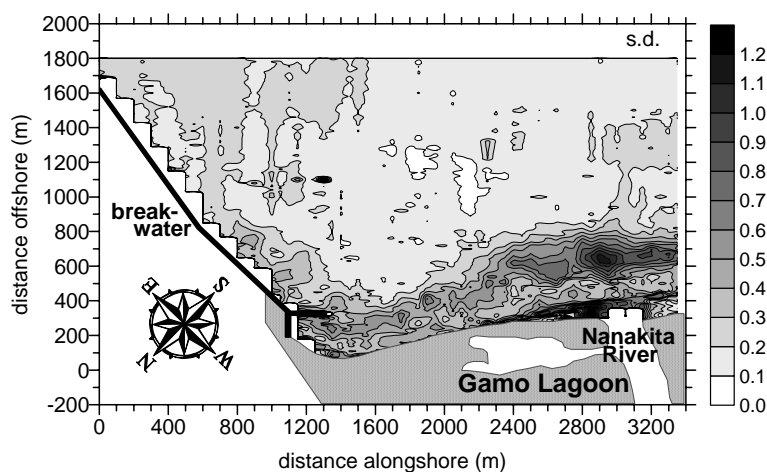


**Figure 3:** Root-mean-squares of bed-elevation variations (contour intervals: 0.1 m).

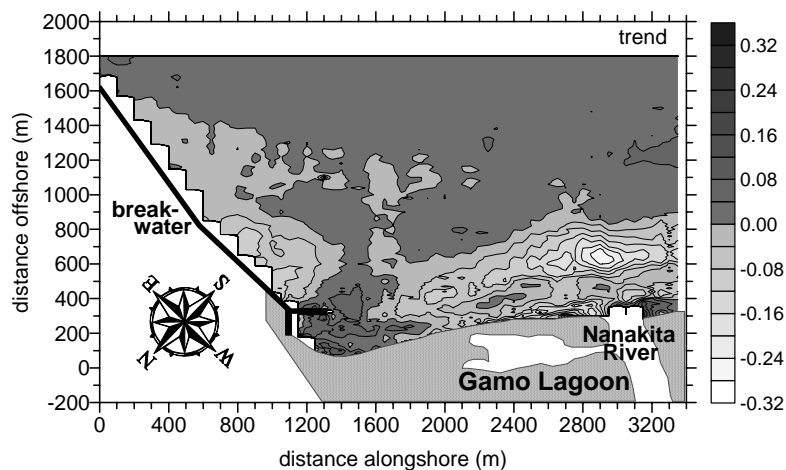


**Figure 4:** Trend of bed elevations (contour intervals: 0.04 m/y).

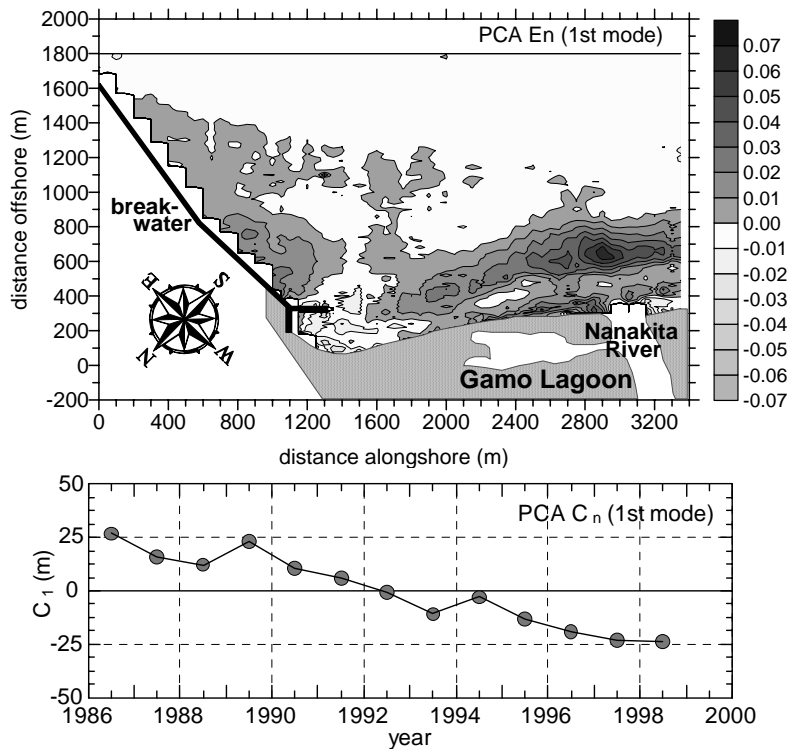


**Figure 5:** Results of the PCA first mode ( $r_1=34.2\%$ ).

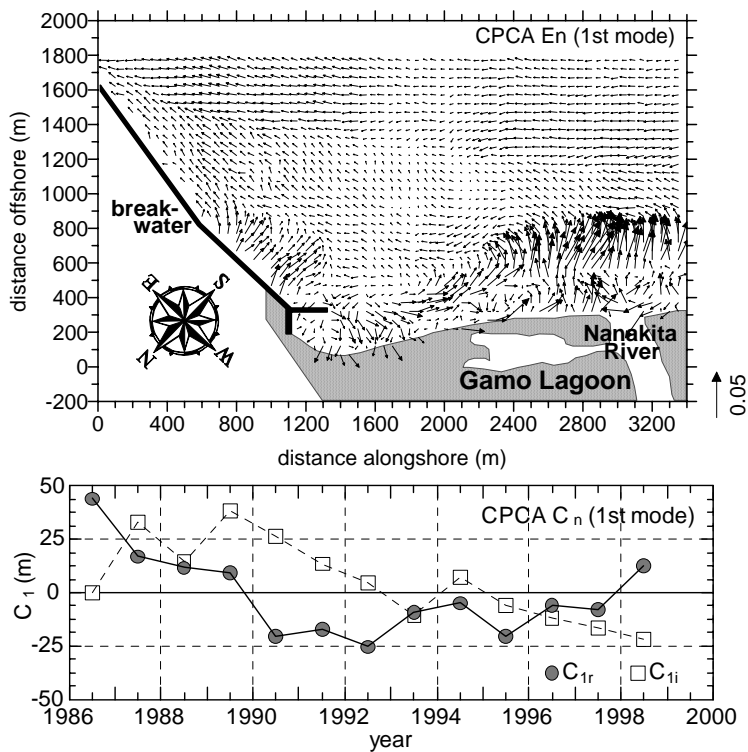


**Figure 6:** Results of the CPCA first mode ( $r_1=44.3\%$ ). In the vector plots of  $e_n$ , real parts are orient vertically upward and imaginary parts are oriented horizontally dextral.

To appear in Proceedings of Coastal Structure 2003, Portland, OR, USA, August 2003 (in print)  
conventional PCA is considerably similar to the trend map, suggesting the PCA is less informative. The complex EOFs (CEOFs) and their temporal weightings,  $c_n(t)$ , appear relatively similar to the results from PCA, however the complex vectorial representations are much harder to us to understand than the PCA outputs.

## Discussion

### (1) The first complex eigenmode

To further investigate the geomorphology of the study area, the bathymetry maps are reconstructed with the first three complex eigenmodes, the CEOFs and the complex temporal weightings, as sequentially displayed for the 12 years in Figure 6. The reconstructed bathymetry using only the first mode (Figure 7 (a)) shows that the seabed near the breakwater is found eroded since the bottom elevation alters from deeper (colored white) to shallower (gray). The area near the breakwater is initially deeper, and then this deeper region propagates toward the river mouth. A submerged delta formed in front of the river mouth has been developed by 1989, and then continuously eroded; the color changes from gray to white.

The offshore waves, bihourly observed by an ultrasonic wave gage (the location is shown as "USW" in Figure 1) at a frequency of 2 Hz, is used to calculate the alongshore and cross-shore components of energy-mean wave energy fluxes (Figure 8). The alongshore energy flux,  $E_{fa}$ , which is well-known to positively correlate with the alongshore sediment transport rate, has a positive peak in between 1989 and 1990, and its average for the whole duration is +214.4 kN/s (i.e., northward). Figure 9 shows spatially-averaged bed elevations calculated from the reconstructed bathymetry solely with the first mode for the six subregions as illustrated in Figure 10. The northward sediment transport largely affects the geomorphology due to the first mode, inducing the erosion of the submerged delta (region 1) and the resulting accretion around the breakwater (region 3) since the breakwater acts as an alongshore sediment trap. The propagation of the deeper region from the region 3 to region 1 shown in Figure 7 (a) thus corresponds to the migration of the accumulated area.

### (2) The second complex eigenmode

The reconstructed bathymetry based on the second mode (Figure 7 (b)) indicates that the deeper region (white) formed offshore of the river outlet in 1986 gradually spread northward in the following two years. Then, the shallower region (gray) appears offshore in 1988, and subsequently propagates landward. The similar cyclic migration of the topography at a period of about 4 years can be also found after 1989. This cyclic behavior exactly coincides with the cyclic fluctuation of the river discharge but has a phase lag (about an year) as shown in Figure 11, suggesting that the sediments previously discharged from the river to the offshore return again into the nearshore region.

### (3) The third complex eigenmode

The spatially-averaged bed elevations for the two nearshore areas (D.L.+1m to -4m and D.L. -4m to -8m) are computed from the reconstructed bathymetry with the third mode (Figure 12). The bed levels definitely fluctuate in response to the cross-shore component of the wave energy flux,  $E_{fc}$ , indicating that the nearshore

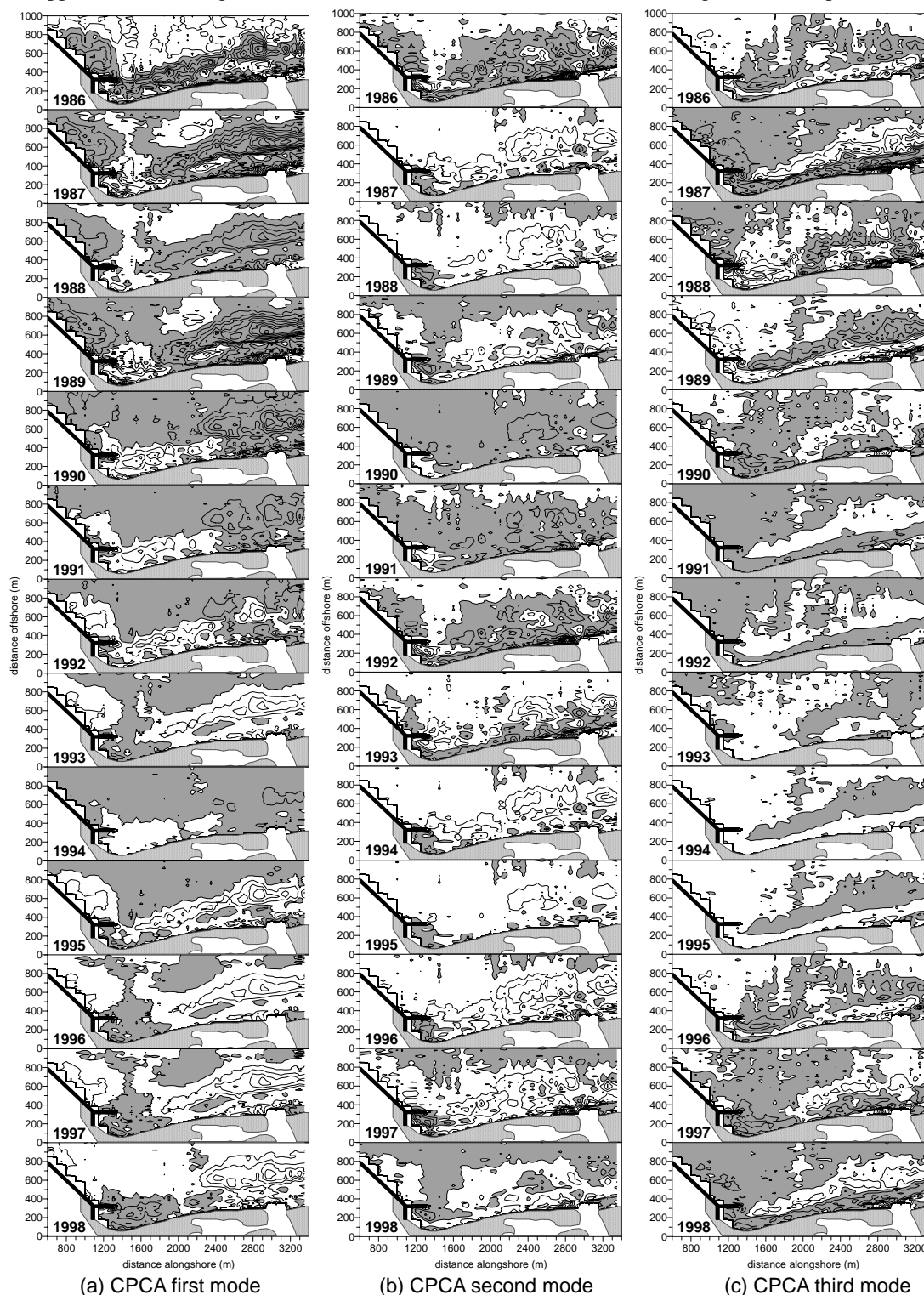


**Figure 7:** Sequential representations of the fluctuating components of the reconstructed bathymetries from 1986 to 1998 based on the CPCA (a) first mode, (b) second mode and (c) third mode. White: regions shallower than the averaged depths displayed in Figure 2, gray: deeper regions. Contour intervals are set to be 0.2m.

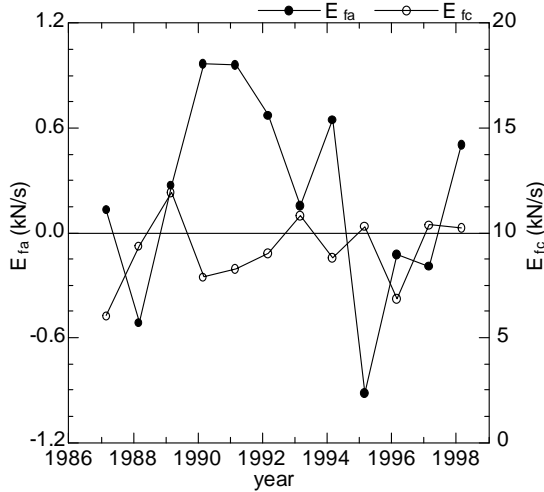


**Figure 8:** Annual variations of the offshore waves. Alongshore component of wave energy fluxes,  $E_{fa}$ , and cross-shore component,  $E_{fc}$ .

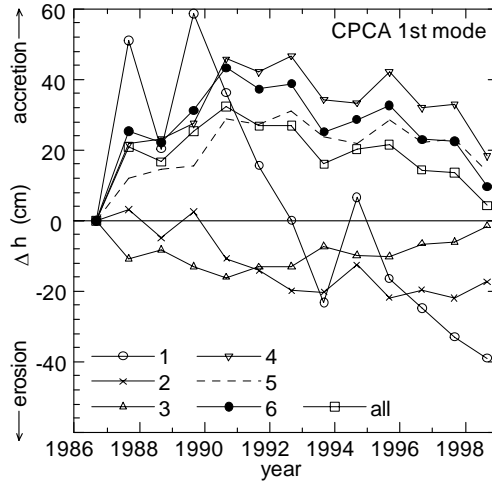


**Figure 9:** Bed level variations of the reconstructed bathymetry computed with the CPCA first mode.

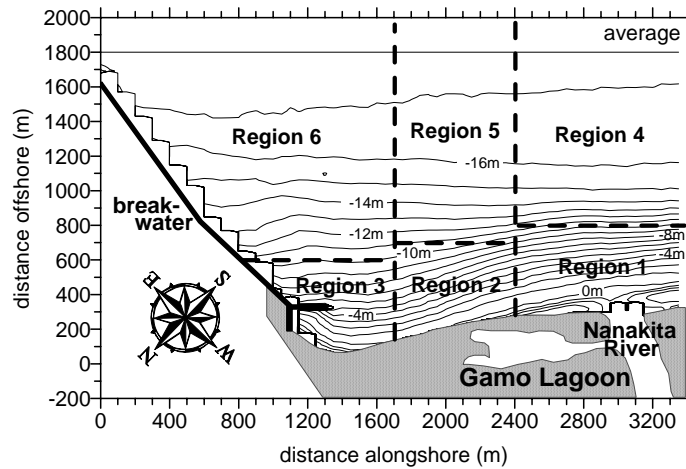


**Figure 10:** Six subregions divided to use for the present analyses.

topography changes driven by the cross-shore sediment transport emerge in the third mode of the CPCA as shown in Figure 7 (c).

#### (4) Complex principal component analysis on beach morphology

While the preliminary investigation using the conventional PCA exhibits standing waves in the topography variations between the breakwater and the river mouth, only the CPCA can describe the southward propagation of the accreted area (in the first mode) and the large-scale cyclic structure of the onshore migration of the bed forms (in the second mode). Hence, the CPCA is expected to be one of the most efficient

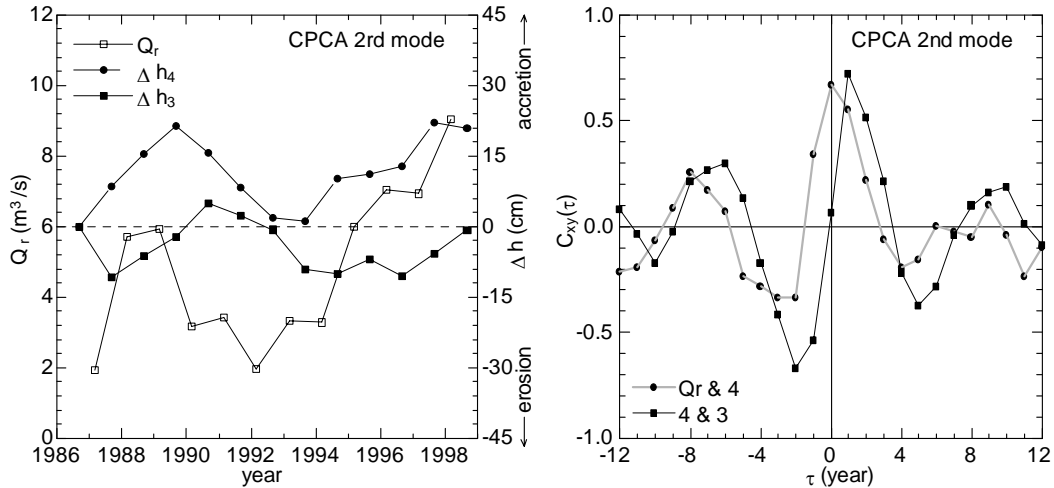


**Figure 11:** River discharge and spatially-averaged bed elevations of subregions 3 and 4 reconstructed with the CPCA second mode. Left: time series, Right: cross-correlation functions.

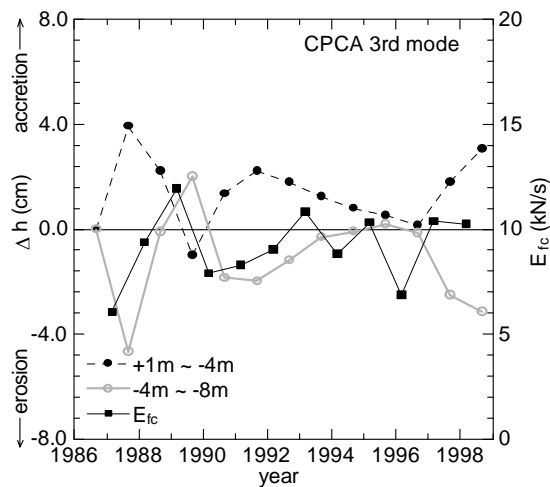


**Figure 12:** The cross-shore component of the wave energy flux and bed elevations of two subregions reconstructed with the CPCA third mode.

and comprehensive methodology for analyzing bathymetry data sets with complicated morphodynamic processes.

## Conclusions

The complex principal component analysis (CPCA) successfully detects significant medium-term geomorphology from the original bathymetric data. The successive erosion of the submerged delta at the Nanakita River estuary and the

To appear in Proceedings of Coastal Structure 2003, Portland, OR, USA, August 2003 (in print)  
resultant accretion near the breakwater due to the northward alongshore sediment transport appears in the first mode. The large-scale coherent structure of the onshore sediment migration induced by the fluvial discharge, and the cross-shore sediment transport due to the wave action are found in the second and the third mode.

## References

- Bosma, K.F. and Darlymple, R.A. (1996). "Beach profile analysis around Indian River Inlet, Delaware, USA", in *Proc. 25<sup>th</sup> Intl. Coastal Eng. Conf.*, Amer. Soc. Civ. Eng., pp.401-405, 1996.
- Horel, J.D. (1984). "Complex principal component analysis: Theory and examples" , *J. Climate Appl. Meteor.* , Vol. 23 , pp.1660-1673.
- Kuriyama, Y. and Lee, J.-H. (2001). "Medium-term beach profile change on a bar-trough region at Hasaki, Japan, investigated with complex principal component analysis", in *Proc. Coastal Dynamics 2001*, Amer. Soc. Civ. Eng., Lund, Sweden, pp.959-968.
- Kuriyama, Y. (2002). "Medium-term bar behavior and associated sediment transport at Hasaki, Japan", *J. Geophys. Res.*, Vol. 107, No. C9, 3132, doi:10.1029/2001JC000899.
- Liang, G. and Seymour, R.J. (1991). "Complex principal component analysis of wave-like sand motions", *Proc. Coastal Sediments '91*, Amer. Soc. Civ. Eng., pp.2175-2186.
- Morishita, Y., Takahashi, J., Kawamata, R., Sakai, T. and Katano, A. (1995). "Beach stabilization by controlling reflected waves due to a port structure" (in Japanese), in *Proc. Coastal Eng.*, Japan Soc. Civ. Eng., Vol. 42, pp.711-715.
- Ruessink, B.G., Wijnberg, K.M., Holman, R.A., Kuriyama, Y. and Van Enckevort, I.M.J. (2003). "Intersite comparison of interannual nearshore bar behavior". *J. Geophys. Res.*, Vol. 108, 3249, DOI:10.1029/2002JC001505.
- Tanaka, N. (1983). "A Study on Characteristics of Littoral Drift Along the Coast of Japan and Topographic Change Resulted From Construction of Harbour on Sandy Beach" (in Japanese), in *Tech. Note of the Port and Harbour Res. Inst.*, No.453, 148p., Port and Harbour Res. Inst., Yokosuka, Japan.
- Tanaka, S., Yamamoto, K., Kamoda, Y., Yanagimachi, T., Onomatu, T. and Gotoh, H. (1995). "Field Measurements of Sediment Transport in the Vicinity of a Fishing Port on the Southern Shore of Sendai Bay" (in Japanese), in *Proc. Coastal Eng.*, Japan Soc. Civ. Eng., Vol.42, pp.666-670.
- Tanaka, H., Takahashi, F. and Takahashi, A. (1996). "Complete Closure of the Nanakita River Mouth in 1994", in *Proc. 25th Int. Conf. Coastal Eng.*, Amer. Soc. Civ. Eng., pp.4545-4556.
- Uda, T., Omata, A. and Minematsu, M. (1990). "Crisis of Sandy Beaches along Sendai Bay Area" (in Japanese), in *Proc. Coastal Eng.*, Japan Soc. Civ. Eng., Vol. 37, pp. 479-483.
- Winant, C.D., Inman, D.L. and Nordstrom, C.E. (1975). "Description of seasonal beach change using empirical eigenfunctions", *J. Geophys. Res.*, Vol.80, No.15, pp.1979-1986.